Cell

Structural Basis for Signal-Sequence Recognition by the Translocase Motor SecA as Determined by NMR

Ioannis Gelis,[1] Alexandre M.J.J. Bonvin,[2] Dimitra Keramisanou,[1] Marina Koukaki,[3] Giorgos Gouridis,[3,4] Spyridoula Karamanou,[3] Anastassios Economou,[3,4] and Charalampos G. Kalodimos[1,*]
[1]Department of Chemistry, Rutgers University, Newark, NJ 07102, USA
[2]Bijvoet Center for Biomolecular Research, Faculty of Science, Utrecht University 3584CH, Utrecht, The Netherlands
[3]Institute of Molecular Biology and Biotechnology, FORTH, PO Box 1385, GR-71110, Iraklio, Crete, Greece
[4]Department of Biology, University of Crete, PO Box 1527, GR-71110, Iraklio, Crete, Greece
*Correspondence: babis@rutgers.edu
DOI 10.1016/j.cell.2007.09.039

SUMMARY

Recognition of signal sequences by cognate receptors controls the entry of virtually all proteins to export pathways. Despite its importance, this process remains poorly understood. Here, we present the solution structure of a signal peptide bound to SecA, the 204 kDa ATPase motor of the Sec translocase. Upon encounter, the signal peptide forms an α-helix that inserts into a flexible and elongated groove in SecA. The mode of binding is bimodal, with both hydrophobic and electrostatic interactions mediating recognition. The same groove is used by SecA to recognize a diverse set of signal sequences. Impairment of the signal-peptide binding to SecA results in significant translocation defects. The C-terminal tail of SecA occludes the groove and inhibits signal-peptide binding, but autoinhibition is relieved by the SecB chaperone. Finally, it is shown that SecA interconverts between two conformations in solution, suggesting a simple mechanism for polypeptide translocation.

INTRODUCTION

Although all proteins are synthesized in the cytoplasm, more than a third is transported to other subcellular compartments or regions, inside a membrane, or to the extracellular milieu (Wickner and Schekman, 2005). The entry of virtually all proteins to the export pathway, both in eukaryotes and prokaryotes, is controlled by a short signal sequence (15–30 residue long), which is typically encoded at the N terminus of the exported protein (Hegde and Bernstein, 2006). The Sec translocase is a highly conserved multipartite protein machinery responsible for handling the vast majority of bacterial and ER-exported proteins (Osborne et al., 2005). In bacteria, protein targeting to the membrane-embedded SecYEG protein-conducting channel is the result of the specific recognition of the signal sequence by either the signal recognition particle (SRP) or SecA, the highly conserved and essential ATPase motor of the translocase (Mitra et al., 2006). How signal sequences interact with any of these receptors is entirely unknown.

Soluble secretory preproteins emerging from the ribosome are captured in an unfolded, translocation-competent state by the SecB chaperone (Randall et al., 1997). The complex is then targeted to SecA, which binds both the signal sequence and the mature domain of the preprotein, as well as SecB (Lill et al., 1990; Randall and Hardy, 2002). SecA couples the export of preproteins through the SecYEG translocon with the expenditure of metabolic energy provided by ATP binding and hydrolysis.

SecA is a large (204 kDa) homodimeric protein (Figure 1A) consisting of 901 residues per protomer (Figure 1B). Its helicase-like motor is located at the N terminus and is assembled by the discontinuous nucleotide-binding domain (NBD) and the intramolecular regulator of ATP hydrolysis-2 domain (IRA2). The nucleotide binds at a cleft formed at the interface of NBD and IRA2 (Sianidis et al., 2001; Hunt et al., 2002). Crosslinking and biochemical experiments have suggested that preproteins and signal sequences interact with the preprotein-binding domain (PBD), which "sprouts" out of the body of NBD through an antiparallel β sheet (Kimura et al., 1991; Kourtz and Oliver, 2000; Papanikou et al., 2005; Musial-Siwek et al., 2007). A number of grooves formed between PBD and other domains have been proposed as potential binding sites for the signal peptide on the basis of structural data of unliganded SecA (Hunt et al., 2002; Osborne et al., 2004). The C-terminal domain of SecA encompasses four substructures: the long α-helical scaffold domain (SD), the IRA1 hairpin, the winged domain (WD), and a flexible, mostly crystallographically unresolved, region (Figure 1B).

Specific interaction between a signal sequence and SecA is a decisive step in correctly sorting secretory

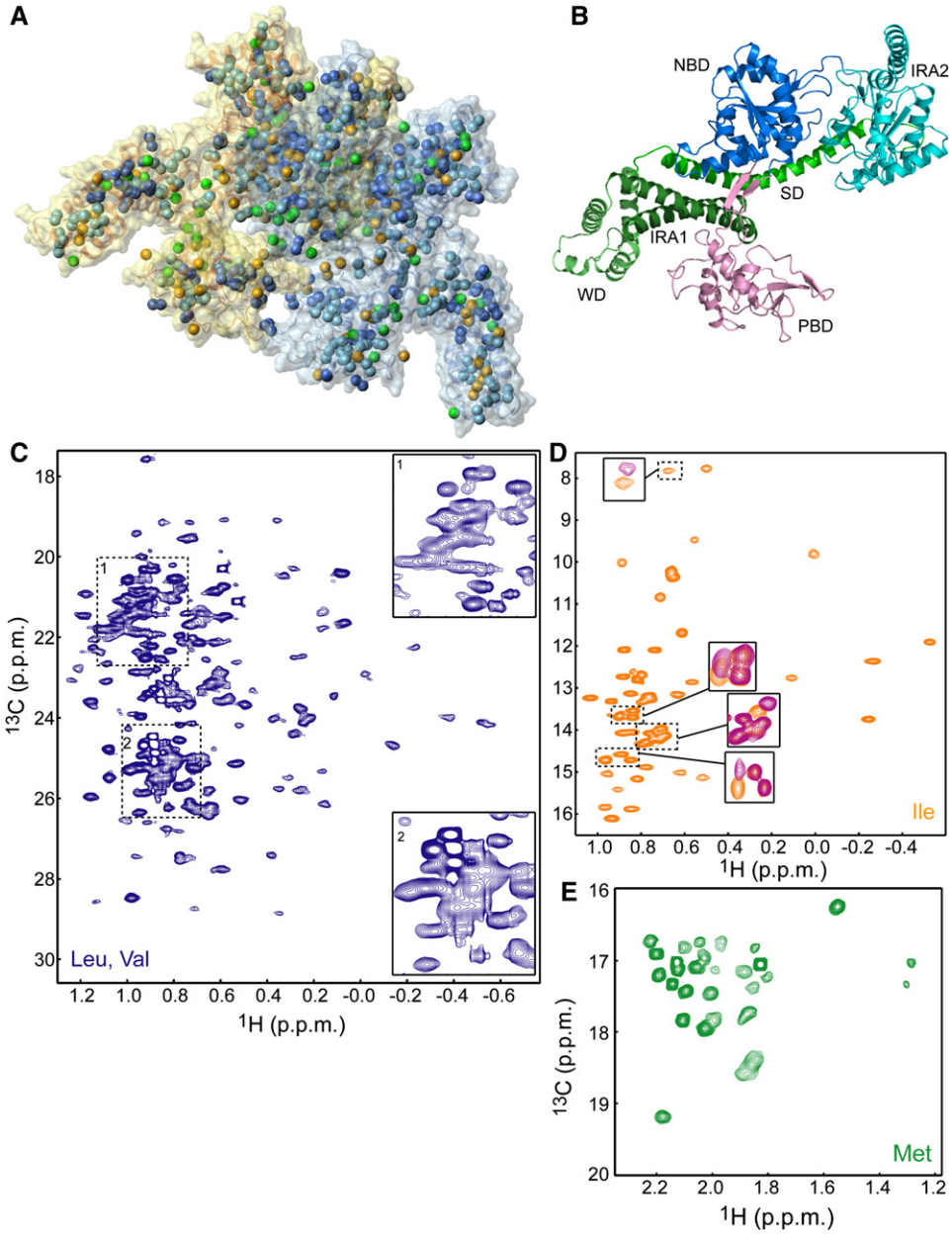

Figure 1. Methyl-TROSY Spectra of the Full-Length 204 kDa SecA

(A) Structural model of dimeric *E. coli* SecA (PDB 2FSF) displayed as a semitransparent solvent-accessible surface. The methyl groups are displayed as spheres. The color code is as follows: Ile, orange (54 residues); Leu, light blue (82 residues); Val, dark blue (59 residues); and Met, green (33 residues). The two protomers are colored differently.

(B) Structural model of one of the protomers of dimeric *E. coli* SecA colored according to domain organization.

(C–E) ^{1}H-^{13}C HMQC spectra of SecA (C) U-[^{2}H,^{12}C],Val, Leu-[$^{13}CH_3$,$^{12}CD_3$], (D) U-[^{2}H,^{12}C], Ile-δ1-[$^{13}CH_3$], and (E) U-[^{2}H,^{12}C], Met-[$^{13}CH_3$]. In (C), expanded views of the crowded areas of the spectrum are shown. In (D), regions of the spectrum of unliganded SecA (orange) are overlaid with the spectrum of SecA bound to the KRR-LamB signal sequence (magenta).

from nonsecretory proteins. As such, this binding interaction must be of extreme fidelity. One of the most intriguing aspects of SecA is its capacity to recognize hundreds of different signal sequences characterized by the lack of any consensus in their primary sequence. Their only common characteristic is a stretch of hydrophobic residues preceded by positively charged residues in the N terminus (von Heijne, 1985; Gierasch, 1989). To date, how SecA accomplishes this challenging task of promiscuous binding remains a conundrum.

Here, we have used NMR spectroscopy to structurally characterize the interaction of full-length SecA with functional signal peptides. By exploiting recent advances in isotope labeling and NMR methodology, we have been able to observe and assign the methyl side chains of a large number of SecA residues. Structure determination of the SecA-signal peptide complex demonstrates that the peptide forms an α-helix and binds by using both its hydrophobic and charged regions into a flexible and elongated groove in SecA. Signal-peptide binding to SecA is restricted by an autoinhibitory mechanism, which is relieved by the SecB chaperone. Interestingly, SecA appears to undergo a large conformational change in solution that might potentially be coupled to the protein translocation mechanism. The combined data not only explain how SecA might achieve the promiscuous recognition of a large set of signal sequences but also provides insight into how the Sec nanomachinery might ultimately be assembled.

RESULTS

Methyl Transverse Relaxation Optimized Spectroscopy of the 204 kDa SecA

To tackle the 204 kDa SecA, we employed recently developed specific labeling schemes (Sprangers et al., 2007) tailored to overcome resonance broadness and overlap. Specifically, we have produced samples with the methyl groups of Ile, Leu, Val, and Met residues of SecA protonated, in an otherwise completely deuterated background (Figure 1A). The methyl groups of these four residues are excellent probes as they are abundant (220 out of the total 901 residues per protomer) and are distributed throughout SecA (Figure 1A). We used methyl transverse relaxation optimized spectroscopy (TROSY) (Sprangers and Kay, 2007) to optimize both sensitivity and resolution. The recorded ^{1}H-^{13}C heteronuclear multiple quantum (HMQC) spectra are of exceptional quality for all four residues (Figures 1C–1E).

The large size of SecA precludes the use of traditional assignment protocols. For this reason, we followed a domain-parsing strategy. Virtually all domains of SecA and a number of fragments comprising contiguous domains have been isolated and characterized by NMR (Figure 2). Assignment of the methyl groups on these relatively small domains was straightforward with standard methodologies (Keramisanou et al., 2006). Comparison of the ^{1}H-^{13}C HMQC spectra of the various domains with that of the full-length SecA demonstrates very good resonance correspondence (Figure 2 and Figure S1 in the Supplemental Data available online). Therefore, the majority of the assignment of methyl crosspeaks performed in the isolated domains and fragments could be readily transferred to the full-length SecA. Assignment was completed (Figure S2) with 3D NOESY spectra recorded on full-length SecA (Figure S1C). We also used mutagenesis to resolve ambiguities that primarily existed for residues located at the interface of domains (Figure S1A).

Structure Determination of the SecA-Signal Peptide Complex by NMR

The well-studied functional signal peptide KRR-LamB, derived from the LamB porin (Wang et al., 1993; Triplett et al., 2001; Chou and Gierasch, 2005), was used. The peptide binds specifically and stoichiometrically to SecA (one peptide per SecA subunit; Figure S3A). The peptide suppresses the ATPase activity and inhibits translocation (Figures S3B and S3C), as expected for a functional signal peptide (Lill et al., 1990). To determine the structure of the complex, we used simulated annealing of the signal peptide in the presence of the X-ray structure of free *E. coli* SecA (PDB code: 2FSF) by using structural information derived from NMR spectroscopy. To obtain distance restraints between SecA and the signal peptide, we used site-directed spin labeling (SDSL). SDSL combined with NMR-detected paramagnetic relaxation enhancement (PRE) rates has been frequently used for determining high-resolution structures of proteins and their complexes with various ligands (Battiste and Wagner, 2000; Gross et al., 2003; Roosild et al., 2005). We introduced a nitroxide spin label to select positions in the peptide and used methyl-TROSY experiments to observe the distance-dependent broadening of the methyl resonances of SecA in the complex (Figure S4). Changes in resonance intensity induced by peptide binding (Figure S5A) were then converted to distances (see Experimental Procedures). Because of the large density of methyl probes close to the peptide-binding site (within $\sim$30 Å), a large number of SecA-signal peptide distance restraints were obtained (Figure S5B).

We engineered spin labels at different positions in the signal peptide by converting a single amino acid to cysteine, on which a nitroxide spin label was attached. We used NMR and isothermal titration calorimetry (ITC) titration of SecA with the mutant and reduced nitroxide-derivatized peptides to assess the effect of the mutations and the presence of the label on peptide binding to SecA (see also below). Placement of the spin label in the helix resulted in altered binding energetics, presumably because of steric clash with the protein. Two positions that were observed to give the most reliable data were K7C at the N terminus and Q25C at the C terminus (Figure 4A). Placement of the spin label in these positions, rather than closer to the termini, significantly decreased the mobility of the spin label, thereby resulting in reduction of nonspecific broadening. The placement of the spin label in two different positions in the N and C terminus of the peptide not only increased the number of distance restraints by roughly 2-fold but also contributed to the better determination of the relative orientation of the peptide bound to SecA.

To determine the structure of the signal peptide in complex with SecA, we used transferred nuclear Overhauser effect spectroscopy (trNOESY) and differential-line-broadening experiments (Matsuo et al., 1999). We probed the conformation of the peptide bound to SecA by measuring NOEs within the peptide in the presence of a small

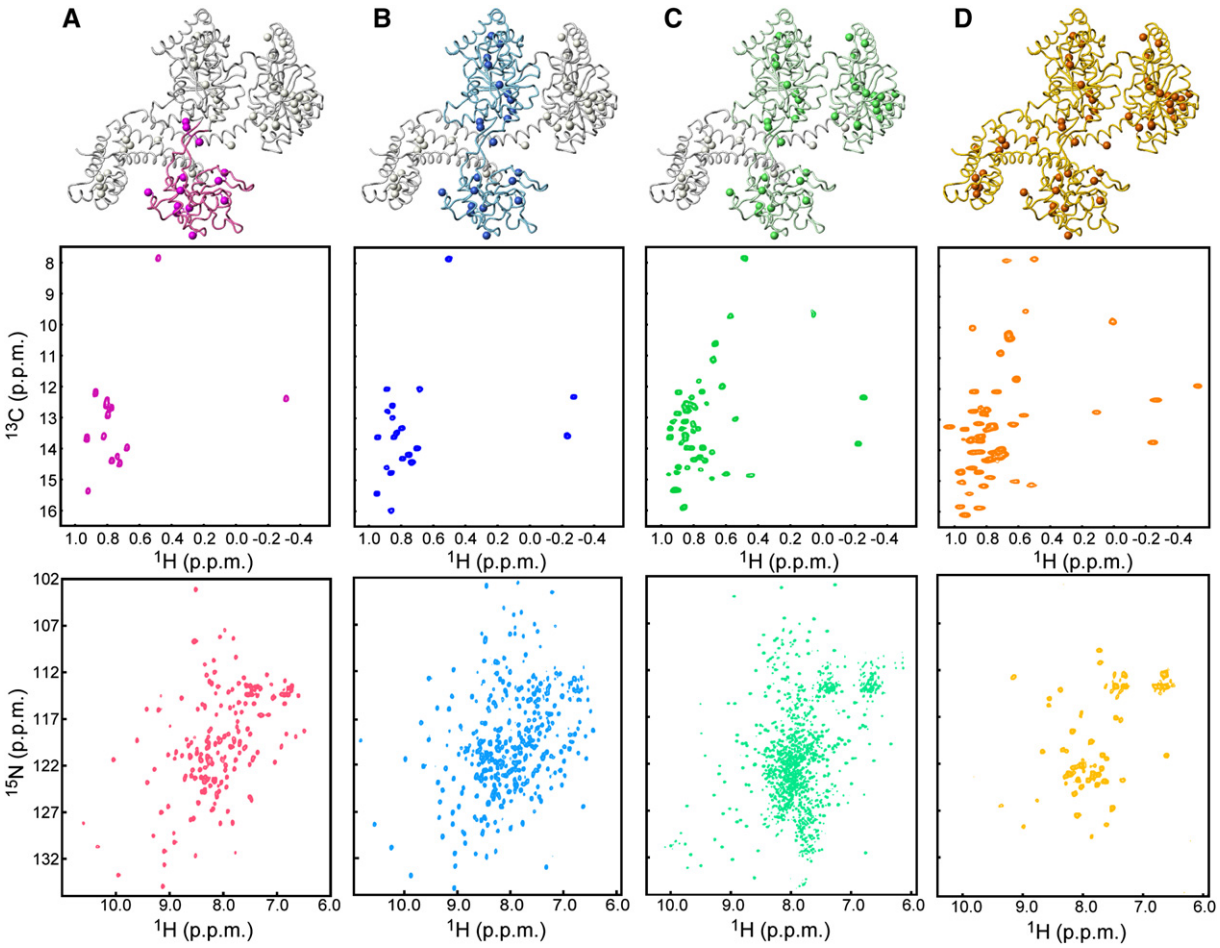

Figure 2. Strategy for the Assignment of Methyl Correlations of SecA

Each column in the figure displays a structural model of one of the protomers of SecA with the domain or fragment studied in isolation being highlighted, along with the corresponding ^{1}H-^{13}C HMQC of Ile-δ1 methyls (displayed as spheres in the model) and the backbone ^{1}H-^{15}N HSQC.

(A) PBD (residues 220–379).

(B) SecAΔC/ΔIRA2 (residues 1–420, comprising NBD and PBD).

(C) SecAΔC (residues 1–610, comprising NBD, PBD, and IRA2).

(D) Full-length SecA (residues 1–901). Only few resonances for the backbone of the full-length SecA are visible (Figure S9).

amount of SecA. In an effort to collect the maximum number of interpeptide NOEs, we extended previous insightful studies (Chou and Gierasch, 2005) by recording NOESY spectra on a 900 MHz spectrometer equipped with a cryoprobe to increase resolution and sensitivity. The data, in agreement with the previous study (Chou and Gierasch, 2005), show that although the free peptide is unstructured, its hydrophobic region (residues Leu13–Val21) adopts an α-helical conformation when interacting with SecA. The structure of the peptide was calculated on the basis of 50 intramolecular NOEs. The family of the best ten structures of the peptide was then used for the determination of the complex that uses the crystal structure of *E. coli* SecA (Papanikolau et al., 2007) as the starting conformation. The structure of the complex was determined on the basis of 162 intermolecular distance restraints. The lowest-energy structure of the complex is shown in Figure 3, whereas the ensemble of the ten best structures is shown in Figure S6.

Signal Peptide Binds into an Expandable and Elongated Groove by using Both Hydrophobic and Electrostatic Interactions

The structural data demonstrate that the signal peptide binds into a relatively large groove formed at the interface of two domains: the PBD and the IRA1 hairpin (Figure 3). The groove consists primarily of PBD residues with a number of IRA1 residues lining only one side of the groove. The groove is mostly hydrophobic but is surrounded by a number of polar and charged residues (Figure 3B). The hydrophobic character of the groove is highly conserved, although the sequence identity of the residues that make up the groove is not (Figure S7).

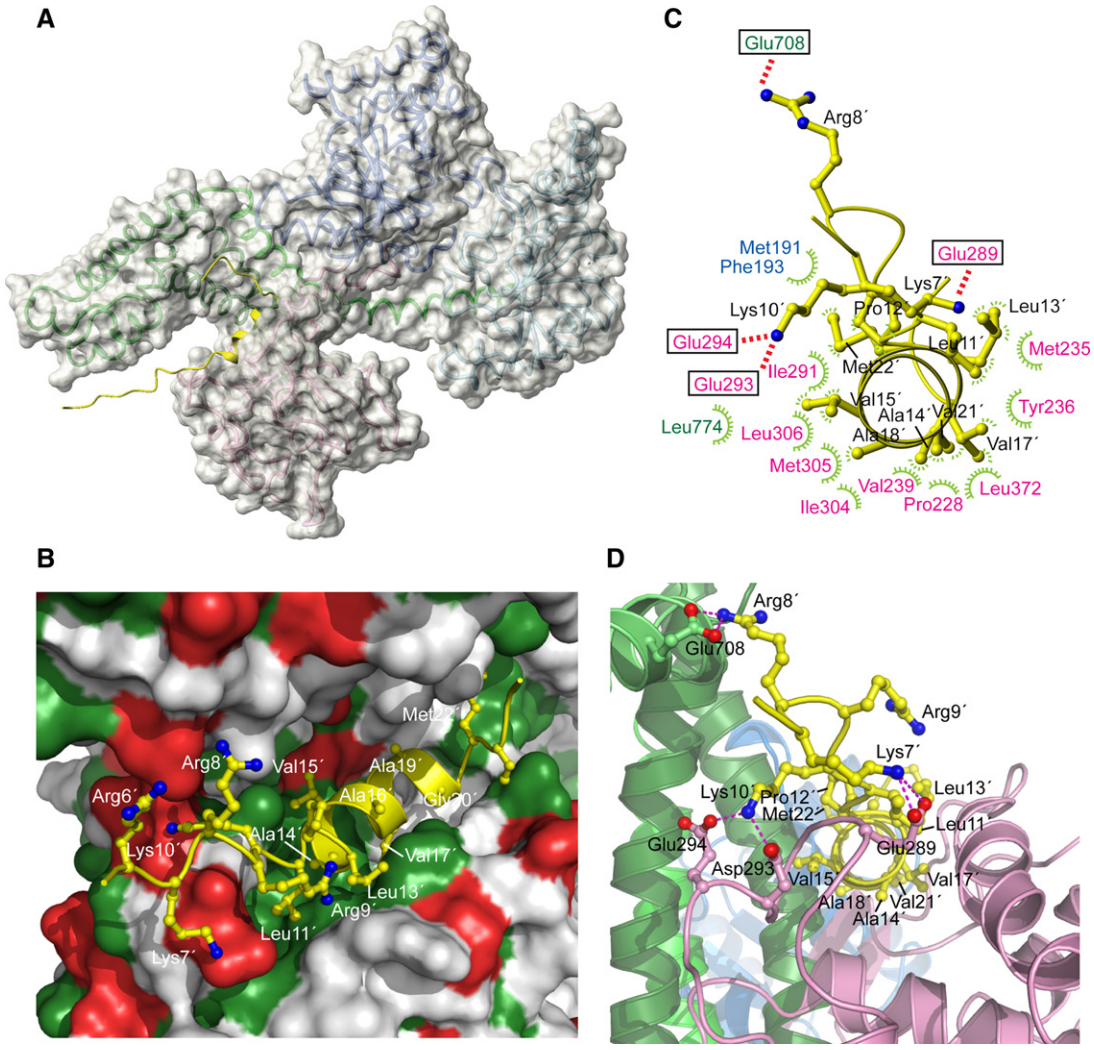

Figure 3. Structural Basis for Signal-Peptide Recognition by SecA

(A) The lowest-energy structure of SecA bound to the KRR-LamB signal peptide is shown. SecA is displayed as a semitransparent solvent-accessible surface, and the signal peptide is shown in yellow. A ribbon model is displayed below the surface (color code is as in Figure 1B).

(B) Closer view of the groove bound to the signal peptide. Green and red surface indicates hydrophobic and acidic residues, respectively. Peptide is shown as a ribbon ball-and-stick representation, and most of its residues are numbered.

(C) Contacts between the peptide (shown in yellow) and SecA residues. Electrostatic and hydrophobic interactions are indicated with red and green lines, respectively. SecA residues are colored according to the domain they are located at.

(D) A view of the groove bound to the signal peptide, wherein SecA is shown in ribbons. The peptide orientation is similar to that in (C). Dotted lines indicate electrostatic interactions between basic peptide residues and acidic SecA residues. Primed numbers indicate peptide residues.

The entire length of the α-helical hydrophobic region of the peptide (consisting of two turns) inserts into the groove, which is relatively long (~28 Å), and thus, it can easily accommodate even longer α helices (Figures 3A and 3B). As expected, hydrophobic interactions between the peptide and SecA dominate the 2500 $Å^2$ (1800 Å nonpolar and 700 Å polar) surface area buried at the SecA-peptide interface. Four short-chain nonpolar aliphatic residues of the peptide (Ala14, Val17, Ala18, and Val21) project toward the center of the hydrophobic face presented by SecA and are completely buried at the interface (Figures 3B–3D). In contrast, longer aliphatic residues (Leu11, Leu13, and Met22, along with Val15) project from the sides of the helix and are partially solvent exposed (Figures 3B and 3D). Together, these residues create a hydrophobic ridge running along the peptide helix axis, forming intimate associations with the predominantly hydrophobic surface of the groove. The face of the peptide α-helix that projects away consists exclusively of short-chain residues, which do not appear to make interactions. These data are in agreement with the differential-line-broadening results showing that the resonances of these residues do not become as broad as those of the other residues of the α-helix.

The positively charged N-terminal residues of the peptide (Lys7, Arg8, Arg9, and Lys10) engage in the formation of salt bridges with acidic residues of SecA located adjacent to the hydrophobic groove (Figures 3B–3D). These residues are seen to interact electrostatically with various acidic residues on SecA in the ensemble of the structures. In any single structure, multiple salt bridges are present, suggesting an important role of these electrostatic interactions in the recognition process. Therefore, the present structural data reveal a dual binding mode for the peptide, which is capable of using both its positively charged N-terminus and the α-helical hydrophobic region to interact with the same groove in SecA.

The C-terminal region of the peptide (residues 24–28), which contains the signal peptidase cleavage site, remains unstructured. This region is not involved in intimate interactions with SecA and is solvent exposed. This picture is in agreement with NOE and differential-broadening data showing that this region remains relatively flexible when bound to SecA.

SecA Uses a Unique Site to Recognize a Variety of Signal Sequences

We used NMR chemical-shift mapping to address whether SecA uses the same groove to recognize various signal sequences. In addition to the KRR-LamB signal peptide used above, three signal peptides from the following preproteins were used: the wild-type LamB, alkaline phosphatase, and M13 procoat (Figure 4A). In all cases, addition of the signal peptide caused significant shift of only a small set of methyl resonances (Figure 1D), suggesting that peptide binding is localized and does not cause global conformational changes to SecA. For example, only four out of the total 54 Ile residues have their chemical shift significantly perturbed upon KRR-LamB signal-peptide binding. Similarly, only a small number of the Val, Leu, and Met methyls are affected. The common set of residues that exhibit the largest shift upon binding of the various signal peptides consists of Ile225, Met235, Val239, Ile291, Met292, Ile304, Met305, Leu306, Val310, and Leu372 at the PDB and Leu774, Met810, and Met814 at the IRA1 hairpin of the C domain. In spite of the diverse amino acid sequence of the peptides, the chemical-shift changes effected by all of them map onto the same region of SecA (Figure 4B). Thus, SecA appears to use the same groove to recognize diverse signal sequences.

Hydrophobic and Electrostatic Interactions Contribute to Signal-Peptide Recognition by SecA

To test the contribution of the hydrophobic contacts on the stability of the complex, we constructed a double SecA mutant wherein two of the most prominent hydrophobic residues of the groove (Ile304 and Leu306) were mutated to Ala (Figures 3C and 4B). The thermodynamic data show that, despite the relatively small perturbation of the hydrophobic surface of the groove, the signal peptide binds with a 6-fold lower affinity to SecA-I304A/L306A than to wild-type SecA (Figures 4C and 4D). This affinity decrease is the result of a large entropic penalty that apparently accompanies the disruption of favorable hydrophobic interactions (Figure 4D).

To assess the contribution of the electrostatic interactions to SecA-peptide binding, we measured the energetics of complex formation in a buffer containing higher salt concentration. Electrostatic interactions are weakened because of the ''screening'' conferred by the salt ions. Indeed, increasing the salt concentration from 40 to 160 mM K^+ caused a 7-fold decrease in the affinity of the peptide for SecA (Figures 4C and 4D). Interestingly, the binding is now purely entropy driven, presumably because it is dominated by hydrophobic interactions. Therefore, both hydrophobic and electrostatic interactions appear to be important for strong binding of the signal peptide to SecA, in accordance with the structural data.

Impairment of the Signal-Peptide Binding to SecA Results in Translocation Defects

To assess the effect of an impaired SecA-signal peptide interaction on the biological function of SecA, we employed in vitro and in vivo experiments. An in vivo genetic complementation experiment indicates that the ability of SecA-I304A/L306A to translocate proteins is compromised (Figure S8). By using a standard in vitro translocation assay, we found SecA-I304A/L306A to be less efficient, by a factor of 8, in its ability to translocate the model preprotein proOmpA into the lumen of SecYEG-containing inverted inner-membrane vesicles (IMVs) when compared to wild-type SecA (Figure 4E). Similarly, IMVs plus preprotein cannot stimulate the basal ATPase activity of SecA-I304A/L306A to the levels seen with wild-type SecA (Figure 4F). The interaction of SecA-bound preproteins with SecYEG is also less efficient in SecA-I304/L306A (Figure 4G). Collectively, our data demonstrate that compromised binding of a signal peptide to SecA results in significant in vivo and in vitro defects during translocation.

The C Tail of SecA Constitutes an Autoinhibitory Element

The extreme C-terminal region of SecA (C tail; residues 834–901 in *E. coli*) is composed of two regions. The first region, consisting of residues 834–855, interacts with the core of SecA and ends up in a β strand (residues 849–854) that forms a β sheet with the two antiparallel β strands linking NBD and PBD (Figure 5A; Hunt et al., 2002). The second region contains a zinc-finger motif that constitutes the primary binding site for the SecB chaperone (Fekkes et al., 1997; Zhou and Xu, 2003). An intriguing aspect of the present structural data is that portion of the peptide-binding groove appears to be occluded by the C tail (Figures 5A and 5B and Figure S9). Indeed, signal-peptide titration to SecA results in displacement of the C tail region that occludes the groove, as evidenced by ^{1}H-^{15}N HSQC spectra (Figure S10). Thus, the binding

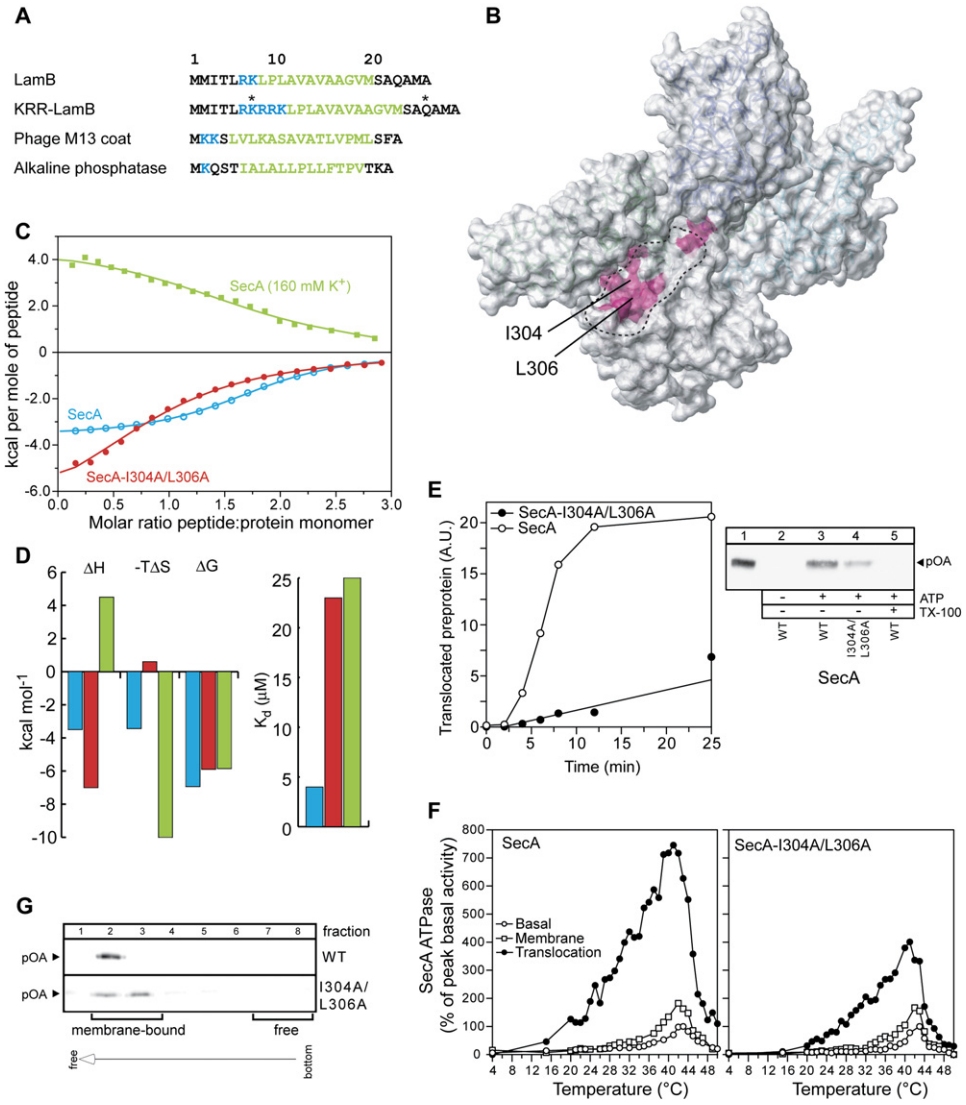

Figure 4. Signal-Peptide Binding to SecA and the Effect of Its Impairment on the Function of SecA

(A) The four different signal sequences used in the present study are shown. In KRR-LamB, the asterisks indicate the positions in which a single Cys mutation was introduced, and this is followed by the incorporation of the nitroxide spin label. Basic and hydrophobic residues are colored blue and green, respectively.

(B) Chemical-shift mapping of the interaction of the signal peptides shown in (A) with SecA. The magenta-colored region indicates the common residues whose chemical shift is significantly affected upon signal-peptide binding (see text for details).

(C) Binding isotherms of the calorimetric titration of the KRR-LamB signal peptide to SecA (open, cyan circles), SecA-I304A/L306A (filled, red circles), and SecA in 160 mM K^+ buffer (green squares). In the first two cases, SecA is in 40 mM K^+ buffer. We mutated Ile304 and Leu306, whose position within the groove is indicated in (B), to assess the relative contribution of hydrophobic interactions in SecA-signal peptide binding, whereas we used higher buffer salt to assess the contribution of electrostatic interactions.

(D) Thermodynamic parameters of the calorimetric titrations in (C) displayed as bars. The color code is as in (C). Weakening of the electrostatic interactions results in hydrophobic interactions being the dominant driving force for complex formation, as suggested by the observation that the reaction becomes enthalpically unfavorable but strongly entropically favorable.

(E) ATP-driven in vitro translocation of proOmpA-His into SecYEG-containing IMVs catalyzed by SecA or SecA-I304A/L306A (right panel). Lane 1 shows 5% of undigested proOmpA-His input. Lane 5 shows that membranes were dissolved with Triton X-100 (1%) prior to proteinase K addition. Proteins were TCA precipitated, analyzed by SDS-PAGE, and immunostained with α-His antibody. The left panel shows the time course of proOmpA translocation kinetics. A total of 20 A.U. corresponds to 1.6 pmol of translocated proOmpA.

(F) k_{cat} values (pmoles Pi/pmol SecA protomer per min) of basal, membrane and translocation ATPase activities of SecA as a function of temperature. Averaged data of three repetitions are shown.

(G) IMV-flotation assay showing weaker binding of proOmpA to SecYEG-bound SecA-I304A/L306A than to wild-type SecA.

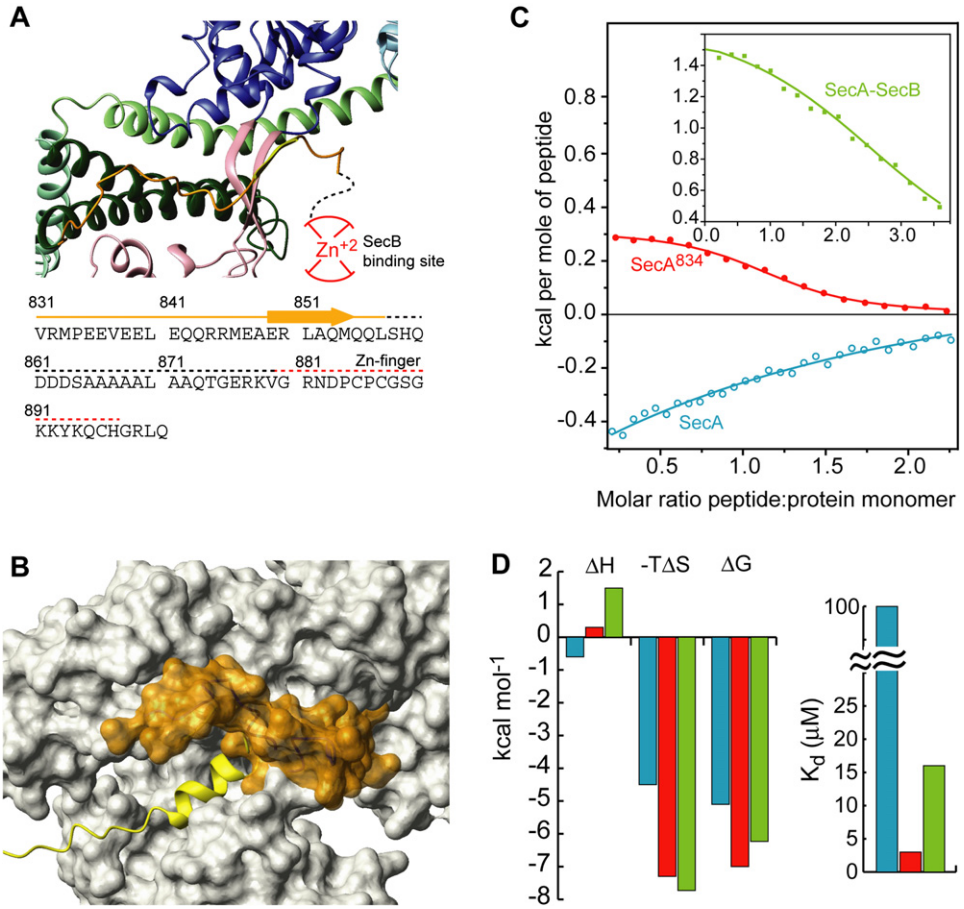

Figure 5. Inhibition of Signal-Peptide Binding by the C Tail of SecA

(A) View of the C tail of *B. subtilis* SecA (PDB 1M6N). This is the only crystal structure wherein part of the C tail is resolved. The *E. coli* SecA sequence of the C tail is shown below the model. Dotted lines indicate crystallographically unresolved regions. Red lines indicate the zinc-finger region, which is the primary SecB binding site.

(B) Structural modeling of the interaction of the C tail in *E. coli* SecA. The C tail is shown in orange surface, and it partially occludes the peptide-binding groove.

(C) Binding isotherms of the calorimetric titration of the wild-type LamB signal peptide to SecA (open, cyan circles), $SecA^{834}$ (filled, red circles), and SecA bound to SecB (green squares).

(D) Thermodynamic parameters of the calorimetric titrations in (C) displayed as bars. The color code is as in (C).

sites for the signal peptide and the C tail are mutually exclusive.

This observation raises the possibility that the C tail might prevent efficient binding of the signal sequence. To test this hypothesis, we determined the thermodynamics of signal-peptide binding to full-length SecA and $SecA^{834}$ (residues 1–834), a deletion construct lacking the entire C tail. The wild-type LamB signal peptide binds to full-length SecA relatively weakly (K_d ~100 μM). Remarkably, removal of the C tail improves binding by more than 30-fold (Figures 5C and 5D). The KRR-LamB peptide binds to full-length SecA relatively strongly (K_d ~3 μM), presumably because of the enhanced charged nature of the N terminus; however, its binding is still improved by a factor of ~10 in $SecA^{834}$. Similarly, binding of the alkaline phosphatase peptide is inhibited by a factor of ~4 (Figure S11). Therefore, the partial occlusion of the peptide-binding groove by the C tail of SecA provides a mechanism for preventing unrestricted access to the signal-peptide-binding groove.

SecB Relieves C Tail-Mediated Autoinhibition

The poor affinity of the wild-type LamB signal peptide for SecA is clearly unexpected, considering that this naturally occurring sequence is functional in vivo. It is noteworthy that, in contrast to most other secretory proteins, LamB-preprotein targeting to SecA in vivo is absolutely SecB dependent (Ureta et al., 2007). Because the primary SecB-binding site lies at the extension of the C tail of SecA, it is conceivable that SecB binding to SecA might displace the C tail, thereby exposing the binding groove to the incoming LamB signal sequence. To test this hypothesis,

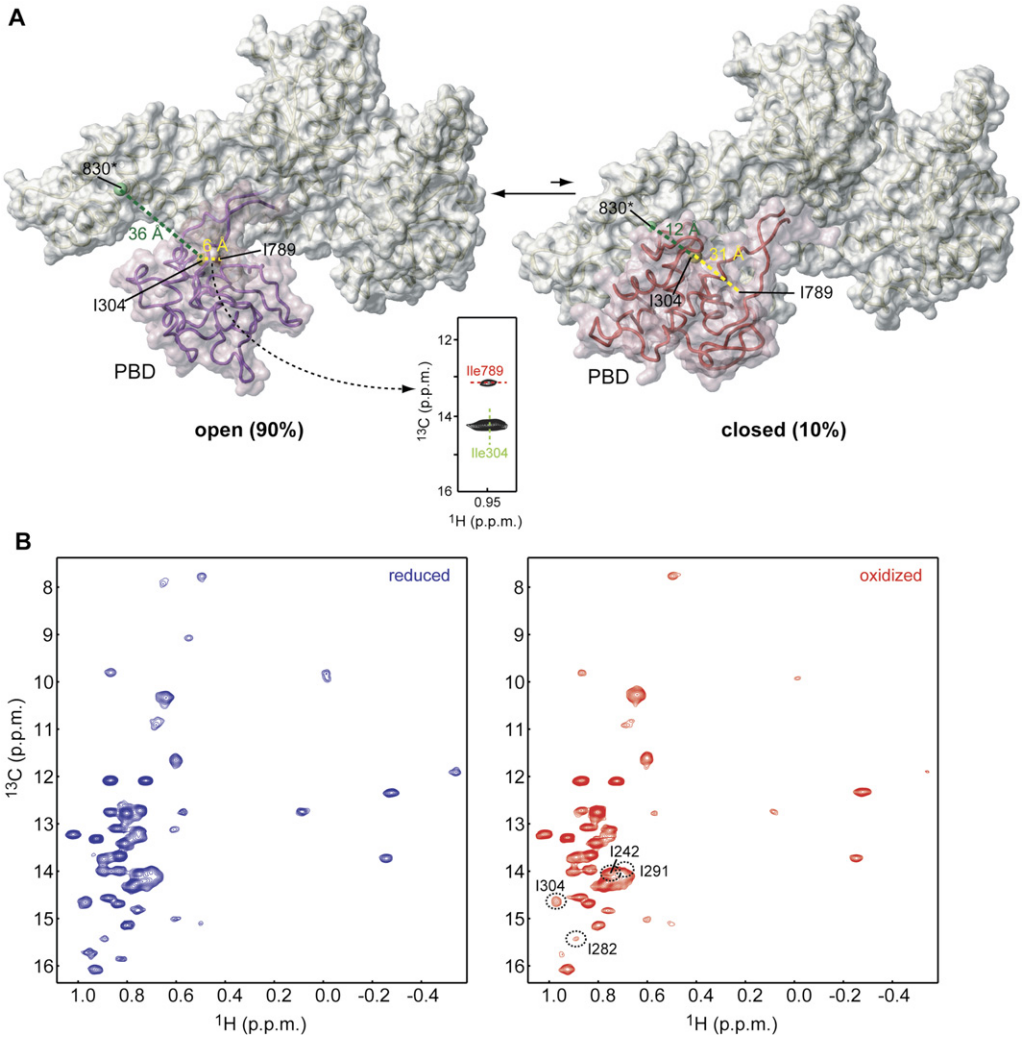

Figure 6. SecA Interconverts between an Open and Closed Conformation in Solution

(A) SecA shown in the so-called open (left) and closed (right) conformations. Interconversion between the two conformations requires that PBD undergo a ~60° rigid-body rotation (Osborne et al., 2004). PBD is displayed as semitransparent surface. The green sphere indicates residue 830, in which a paramagnetic spin label was introduced. Residues Ile304 and Ile789 are shown as yellow and red spheres, respectively. Characteristic distances in the two conformations are indicated. A strong NOE between Ile304 and Ile789 was observed, demonstrating that SecA adopts predominantly the open conformation in solution.

(B) Overlaid ^{1}H-^{13}C HMQC spectra of SecA bearing a spin label in position 830 in the reduced (blue) and oxidized (red) state. Residues that approach the spin label, even transiently, experience a broadening effect, which is suppressed in the reduced state.

we measured the energetics of LamB signal-peptide binding to SecB-bound SecA. Interestingly, in the presence of SecB, LamB signal peptide binds to SecA with a much higher affinity (7-fold increase; Figures 5C and 5D). Thus, SecB appears to counteract the autoinhibitory conformational arrangement, thereby resulting in stronger signal-peptide binding.

SecA in Solution Interconverts between an Open and Closed Conformation

An interesting aspect that has emerged from the various crystal structures of SecA proteins is that PBD can adopt two very different conformations (Figure 6A). In the so-called closed conformation, PDB interacts extensively with the C domain forming a compact structure (Hunt et al., 2002; Sharma et al., 2003; Vassylyev et al., 2006). In contrast, in the "open" conformation, PDB undergoes a ~60° rigid-body rotation resulting in minimal interaction with the C domain and exposing most of PDB surface to the solvent (Osborne et al., 2004; Papanikolau et al., 2007). Crystal-packing effects could selectively favor one of the two forms. Currently, it is unknown which is the most stable PBD conformation in solution.

To determine the relative PBD conformational state in solution, we examined the NOESY data of SecA. An NOE crosspeak was readily assigned between the methyl

groups of Ile 304 and Ile789 (Figure 6A). This is compatible only with the open conformation, wherein the two methyl groups are within 6 Å, and not with the closed conformation, wherein they are located greater than 30 Å apart (Figure 6A). Thus, the NOE data provide strong evidence that the PBD of SecA is in the open conformation in solution.

To gain further insight, we used SDSL to determine interdomain PBD-C domain distances. A spin label was introduced at position 830, located in the end of the IRA1 hairpin (Figure 6A), where the presence of a paramagnetic center would differentially affect the intensity of the methyl probes in the two conformations. For example, the distance to the spin label in position 830 from PBD residues 242, 282, 291, and 304 would be 16 Å versus 44 Å, 13 Å versus 43 Å, 15 Å versus 24 Å, and 12 Å versus 36 Å, in the closed and open conformation, respectively.

If SecA spent 100% of the time in the open conformation, then the presence of a paramagnetic center at position 830 would have absolutely no effect on the intensity of the above group of methyl resonances of PBD residues. However, even methyls that are greater than 40 Å away from the spin label in the open conformation, but very close to the spin label in the closed conformation, are weakly affected (Figure 6B). For example, the intensity of the I304 methyl resonance is reduced by ~30% in the presence of the spin label in position 830, despite the fact that it lies 36 Å apart from the paramagnetic center in the open conformation (Figures 6A and 6B). Similar changes in the intensity were also observed for residues 242, 282, and 291. The intensity loss is fully recovered in the reduced state, suggesting that the intensity decrease of these residues in the paramagnetic sample is due to the, apparently transient, proximity of residue 304 to the spin center at position 830 (Figure 6). As has been elegantly shown recently (Iwahara and Clore, 2006; Volkov et al., 2006; Tang et al., 2006), PRE rates are extremely sensitive to the presence of transiently populated excited states. The estimated PRE rates of the methyl of Ile304 are ~0 and 400 s^{-1} for the open and closed state, respectively. Therefore, our results suggest that the closed conformation represents ~10% of the total population. Overall, the combined NOE and PRE data argue that SecA interconverts in solution between an open conformation, the major form, and a closed conformation, the minor form.

DISCUSSION

Molecular understanding of the translocation process necessitates determination of the structural and dynamic basis for the assembly of the entire Sec translocase machinery. Toward this goal, we have undertaken a challenging NMR study aiming at the structural characterization of the 204 kDa SecA motor ATPase and its interaction with signal peptides. The specific recognition of the N-terminally fused signal sequence by SecA is arguably the most decisive step in correctly targeting secretory polypeptides. The use of specific labeling schemes (Sprangers et al., 2007) and domain-parsing approaches for resonance assignment, combined with paramagnetic spin labeling and relaxation enhancement measurements, enabled the structure determination of this large complex. We anticipate that similar strategies will render other large macromolecular complexes tractable to structural characterization by NMR.

A central feature of the recognition process is the transition of the peptide hydrophobic region from a random-coil conformation to an α-helix upon its interaction with SecA (Figure 3; Chou and Gierasch, 2005). This helix inserts into the relatively deep groove, and almost all of its residues are involved in intimate interactions with the hydrophobic surface of the groove. A similar mechanism appears also to be used by the Tom20 import receptor to bind its signal sequences (Abe et al., 2000). Different signal sequences cause similar chemical-shift perturbation patterns (Figures 4A and 4B), suggesting that SecA uses this groove to recognize the hundreds of different protein substrates. The binding groove has several distinct features: (1) It is quite long (~28 Å), thus explaining how SecA can accommodate signal sequences with much longer α-helical hydrophobic regions. (2) It consists of hydrophobic residues and is surrounded by acidic ones, thereby permitting the signal peptide to bind in a dual mode. This observation explains previous results highlighting the important role of both the hydrophobic and positively charged regions of the peptide (Akita et al., 1990; Mori et al., 1997; Wang et al., 2000; Karamyshev and Johnson, 2005). Both recognition modes contribute greatly to the binding because impairment of the hydrophobic or electrostatic contacts between SecA and the signal peptide results in weaker interaction and significant translocation defects (Figures 4C–4G and Figure S8). Clearly, the extent to which different signal peptides rely on these recognition modes can vary. (3) The binding groove is relatively deep and many small pockets are present at its sides. Hence, it can accommodate signal sequences of varying length and bulkiness of side chains. (4) The groove is lined with several loosely packed methyl groups and Met residues, whose side chain is particularly flexible. These provide a malleable hydrophobic surface that can adapt itself to the binding of signal sequences of varying dimensions. (5) The groove is formed at the interface of two domains, PBD and IRA1. Thus, it is anticipated that the binding site will be quite flexible and expandable by small rearrangement of the domains. Such a rearrangement would give rise to grooves of somehow varying dimensions and expose surfaces of variable amino acid composition. Indeed, inspection of the structural ensemble (Figure S6) suggests that such small rearrangements are energetically allowed. Collectively, the structural plasticity of the binding groove at both the level of the individual side chains and the orientation of the involved domains might be crucial for SecA to recognize its surprisingly diverse range of substrates.

An interesting finding in the present study is that the C tail of SecA partially occludes the peptide-binding groove,

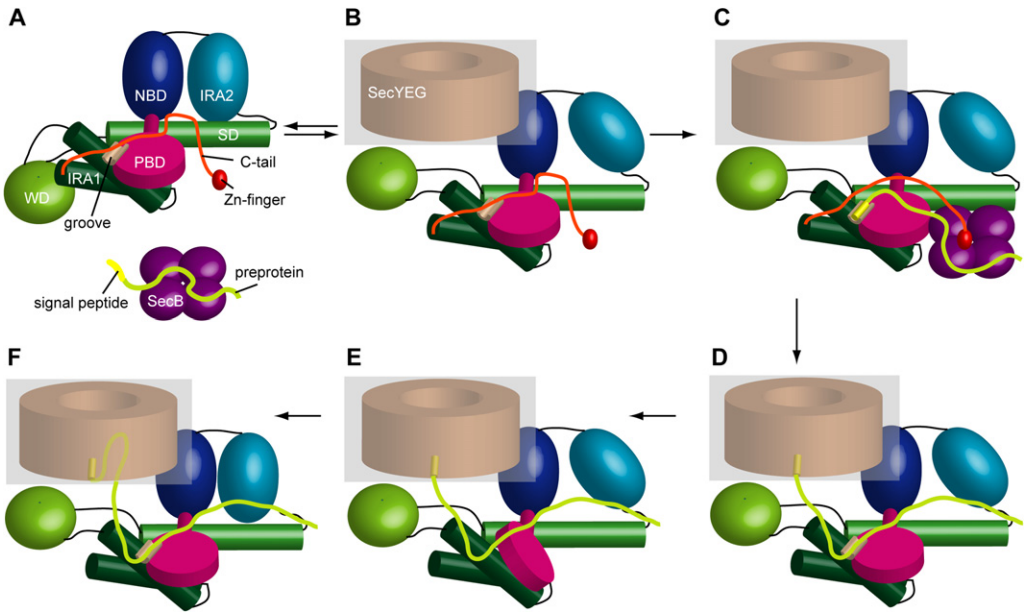

Figure 7. Model of the SecA-Mediated Preprotein Translocation

PBD is shown in the closed state in (E) and in the open state in (A)–(D) and (F). The C tail is not shown in (D)–(F) for clarity. See text for details.

thereby forming the basis of an autoinhibitory mechanism. Intriguingly, the binding of the wild-type LamB signal peptide to SecA is strongly inhibited, but sufficient binding is restored in the presence of the SecB chaperone. Apparently, SecB binding to the zinc-finger site located at the extension of the C tail somehow displaces the C tail from the binding groove, allowing for a stronger SecA-signal peptide interaction. This finding might explain why export of LamB is SecB dependent (Ureta et al., 2007). Because the C tail masks only a portion of the binding groove, it is expected that the extent of signal-peptide-binding inhibition will depend on the exact positioning of the peptide along the elongated groove. This is indeed seen with the alkaline phosphatase peptide, whose binding is inhibited by only a factor of ~4. In this case, the signal sequence will counteract the autoinhibitory conformation, and no additional factors, such as SecB, are needed to relieve autoinhibition. The role of this autoinhibitory mechanism in SecA might be 2-fold. First, it might prevent the untimely interaction of a preprotein with SecA, unless the ternary complex with SecB has formed. Second, it might safeguard against nonspecific binding by acting as a selectivity barrier to ensure that only genuine signal sequences on secretory proteins will have the affinity to overcome it.

The combined NOE and PRE NMR data show that SecA interconverts between an open (major form, 90%) and a closed conformation (minor form, 10%) in solution (Figure 6), which correspond to the two alternative conformations seen in crystal structures (Hunt et al., 2002; Osborne et al., 2004; Papanikolau et al., 2007). Intriguingly, although the PDB part of the groove is accessible in both states, the complete peptide-binding groove forms only in the open state. It is conceivable that the equilibrium of the two extreme conformations might shift as a result of preprotein or SecYEG binding and possibly also during the ATPase cycle. In this case, the large conformational change undergone by PBD might be a functional one, linking preprotein binding to the catalytic cycle, thus, presenting a simple translocation mechanism (see below).

On the basis of the present and previous results, we put forward a refined model of SecA-mediated translocation (Figure 7). SecA partitions between the cytosol and the membrane (Mori et al., 1997). In solution, SecA adopts a catalytically inactive, ADP-liganded state, wherein strong domain-domain interactions prevail (Figure 7A; Sianidis et al., 2001; Fak et al., 2004). Binding to SecYEG at the membrane incurs a loosening of these interactions, thereby causing marginal ATPase stimulation. Although exactly how SecA interacts with SecYEG remains to be determined, both the NBD and the C domain appear to be involved (Mori and Ito, 2006; Osborne and Rapoport, 2007). The peptide-binding groove remains partially masked by the C tail. In the next step (Figure 7C), the SecB-preprotein complex is targeted to SecA. SecB binding to the zinc finger at the end of the C tail somehow displaces the C tail from the groove, thereby relieving autoinhibition. The signal peptide then binds into the groove and adopts an α-helical conformation. Next, SecB is released and the preprotein is transferred entirely to SecA (Figure 7D). Because of the polarity of signal-peptide binding to SecA, the mature domain will likely be directed toward the helicase motor and might bind by bridging the two motor domains (Figure 7D and Figure S12). In such a case, we hypothesize that SecA will bind its protein substrate in a way similar to that by which the Vasa helicase binds its RNA substrate (Sengoku et al., 2006). In this mode of

binding, the preprotein might open further apart the motor domains, explaining why preprotein is required for maximal stimulation of the ATPase activity (Karamanou et al., 2007). In the first step of the actual translocation, the signal peptide will dissociate from SecA and insert into SecYEG, in a step that probably requires ATP hydrolysis (Schiebel et al., 1991; Wang et al., 2004). This transfer is quite favorable because the positively charged N terminus of the peptide interacts with the negative charge of the membrane. For the actual translocation process to work (Figures 7E and 7F), we conjecture that two mechanisms should proceed in synergy. The first one is the closure and opening of the motor, which will be directly regulated by ATP binding, hydrolysis, and ADP release (Keramisanou et al., 2006). Such a movement would constantly push the preprotein forward toward the membrane. The motor motion could potentially be coupled to a second mechanism involving the large conformational change undergone by PBD. Because of its structural and physicochemical properties, the peptide-binding groove is an excellent candidate for binding also the mature portion of the preprotein. We could envision that the two states, open and closed, would have different affinity for the preprotein because the binding groove forms only in the open state. Such a simple mechanism might be sufficient to carry out the translocation process. Intimate association of SecA to SecYEG ensures that these SecA motions also direct corresponding movements of SecYEG that will allow the protein-conducting channel constriction (Van den Berg et al., 2004) to tighten and loosen around the translocated preprotein.

EXPERIMENTAL PROCEDURES

Protein Preparation

His-tagged *E. coli* SecA, SecA^{834}, SecAΔC, SecAΔC-ΔIRA2, and SecAC (34 kDa, residues 611–901) and isolated PBD and IRA2 domains were constructed as described previously and transformed in BL21DE3/pLysS (Sianidis et al., 2001; Keramisanou et al., 2006). Cultures for full-length SecA and its mutants were grown at 30°C, and protein synthesis was induced by addition of 0.5 mM of IPTG at A_{600} ~0.3. Cells were harvested at A_{600} ~0.75. For isotope labeling, minimal media containing $^{15}NH_4Cl$ and [^{2}H,^{12}C] or [^{2}H,^{13}C]-glucose in 99.9% $^{2}H_2O$ were used. For the production of U-[^{2}H],Ile-δ1-[$^{13}CH_3$] and Val,Leu-[$^{13}CH_3$,$^{12}CD_3$] samples, 50 mg l^{-1} of alpha-ketobutyric acid (methyl-$^{13}CH_3$) and 100 mg l^{-1} of alpha-ketoisovaleric acid (dimethyl-$^{13}CH_3$,$^{12}CD_3$) were added to the culture 1 hr prior to addition of IPTG. We produced met-[$^{13}CH_3$] labeled samples by supplementing the medium with 250 mg l^{-1} of [$^{13}CH_3$]- methionine (no side chain scrambling takes place with Met). All protein samples were purified over a nickel-chelating column, and this was followed by ion exchange and gel filtration.

To produce MTSL-derivatized SecA, we constructed the SecA^{834}-Q830C mutation (we used the SecA^{834} construct to avoid crosslinking to Cys residues of the Zn finger). The only other Cys in SecA (Cys98) is not reactive, as judged by the Elman's test and NMR, and therefore it was not mutated. After purification, the protein was exchanged to phosphate buffer (50 mM KPi and 50 mM KCl [pH 8.0]), free of any reducing agent, and it was concentrated (~8 μM). MTSL was added from a concentrated stock in acetonitrile at a 10-fold excess, and the reaction was let to proceed at 4°C for ~12 hr. The completion of the reaction was confirmed by mass spectrometry. Excess MTSL was removed by extensive dialysis with an Amicon stirred cell, and the pH was corrected to 7.5.

Peptide Preparation

All peptides were chemically synthesized by GeneScript (Piscataway, NJ). To crosslink the KRR-LamB cysteine mutants with MTSL, we dissolved the peptides in phosphate buffer (25 mM KPi and 5 mM KCl [pH 8.0]) at a concentration of ~0.1 mM, and MTSL was added in a 10-fold excess. Complete crosslinking was verified by mass spectrometry. Excess MTSL was removed by extensive dialysis with an Amicon stirred cell, and the pH was corrected to 7.5.

NMR Spectroscopy

NMR experiments were performed on Varian 600 and 800 MHz and Bruker 900 MHz spectrometers. Sequential assignment of the ^{1}H, ^{13}C, and ^{15}N protein backbone chemical shifts for isolated domains and fragments was achieved by means of throughbond heteronuclear scalar correlations with standard pulse sequences. Methyl group assignment was accomplished with 3D (H)C(CO)NH, 3D H(C)(CO)NH, and 3D ^{15}N- or ^{13}C-edited NOESY-HMQC spectra. All NMR samples were prepared in 50 mM KCl, 50 mM potassium phosphate, 1 mM DTT, and 1 g l^{-1} NaN3 (pH 7.5). Concentrations were 0.3 mM for full-length SecA and 0.3-0.8 mM for the various constructs. Spectra were recorded at 25°C. Under these conditions, SecA in the presence or absence of the signal peptide is dimeric (Figure S13).

Determination of Distance Restraints from PREs

We determined PRE-derived distances from methyl-TROSY spectra of SecA by measuring peak intensities before (paramagnetic) and after (diamagnetic) reduction of the nitroxide spin label with ascorbic acid. PRE values were then converted to distances by a modified Solomon-Bloembergen equation for transverse relaxation, as described previously (Battiste and Wagner, 2000). Two sets of restraints were incorporated into subsequent structure calculations. Methyl groups strongly affected by the presence of the spin label in the peptide (I_{para}/I_{dia} < 0.15) and whose resonances broaden beyond detection in the paramagnetic spectrum were restrained with only an upper-bound distance estimated from the noise of the spectrum and an addition of 4 Å. Methyl groups whose resonances appear in the paramagnetic spectra (I_{para}/I_{dia} < 0.85) were restrained as the calculated distance with ±4 Å upper/lower bounds. For the peptide with the MTSL at residue position 7 and 25 and position 66 and 96 (162 in total), intermolecular restraints were determined (see Supplemental Experimental Procedures).

Structure Calculation

The structure of the SecA-KRR-LamB signal peptide was calculated with CNS (Brunger et al., 1998), within HADDOCK 2.0 (Dominguez et al., 2003). The crystal structure of *E. coli* SecA (Papanikolau et al., 2007) was used as the starting conformation of SecA. For the signal peptide, a helical structure was imposed for residues L13 to M22 of the hydrophobic core on the basis of transferred NOESY data of the peptide bound to SecA, whereas the positively charged N terminus and the polar C terminus were unrestrained. The PRE-derived intermolecular distances were introduced as unambiguous restraints. In addition, we used the chemical-shift perturbation data for methyl groups of SecA to define ambiguous interaction restraints. The solutions were clustered with a 3.0 Å RMSD cutoff criterion (the RMSD refers to the peptide backbone atoms calculated after fitting on SecA backbone atoms). The twenty lowest-score structures of the lowest score cluster were selected for analysis (see Supplemental Experimental Procedures).

ITC Experiments

All calorimetric titrations were performed on a VP-ITC microcalorimeter (Microcal). Protein samples were extensively dialyzed against the ITC buffer containing 20 mM KPi (pH 7.5), 20 mM KCl, and 1 mM

TCEP. We prepared the ligand solution by dissolving peptide in the flow through of the last buffer exchange. Hydrophobic peptides were first dissolved in 100% DMSO and then transferred stepwise to the ITC buffer at a final concentration of 2%–4% DMSO. We also added DMSO at the same concentration to the protein solution to match the buffer composition of the peptide. The data were fitted with Origin 7.0 (Microcal).

Supplemental Data

Supplemental Data include additional Experimental Procedures and 13 figures and are available online at http://www.cell.com/cgi/content/full/131/4/756/DC1/.

ACKNOWLEDGMENTS

We are grateful to B. Pozidis for the MALLS data, S. Backo and O. Uchime for assistance with sample preparation, and R. Ghose for useful discussions. This work was supported by U.S. National Institutes of Health grant GM-73854 (to C.G.K.), by a Scientist Development Grant from the American Heart Association (to C.G.K.), and by the European Union (grant LSHG-CT-2005-037586 to A.E.) and the Greek General Secretariat of Research and the European Regional Development Fund (grants 01AKMON46 and PENED03ED623 to A.E.). G.G. is an Onassis Foundation predoctoral fellow.

Received: June 4, 2007
Revised: July 30, 2007
Accepted: September 28, 2007
Published: November 15, 2007

REFERENCES

Abe, Y., Shodai, T., Muto, T., Mihara, K., Torii, H., Nishikawa, S., Endo, T., and Kohda, D. (2000). Structural basis of presequence recognition by the mitochondrial protein import receptor Tom20. Cell *100*, 551–560.

Akita, M., Sasaki, S., Matsuyama, S., and Mizushima, S. (1990). SecA interacts with secretory proteins by recognizing the positive charge at the amino terminus of the signal peptide in Escherichia coli. J. Biol. Chem. *265*, 8164–8169.

Battiste, J.L., and Wagner, G. (2000). Utilization of site-directed spin labeling and high-resolution heteronuclear nuclear magnetic resonance for global fold determination of large proteins with limited nuclear overhauser effect data. Biochemistry *39*, 5355–5365.

Brunger, A.T., Adams, P.D., Clore, G.M., DeLano, W.L., Gros, P., Grosse-Kunstleve, R.W., Jiang, J.S., Kuszewski, J., Nilges, M., Pannu, N.S., et al. (1998). Crystallography & NMR system: A new software suite for macromolecular structure determination. Acta Crystallogr. D Biol. Crystallogr. *54*, 905–921.

Chou, Y.T., and Gierasch, L.M. (2005). The conformation of a signal peptide bound by Escherichia coli preprotein translocase SecA. J. Biol. Chem. *280*, 32753–32760.

Dominguez, C., Boelens, R., and Bonvin, A.M. (2003). HADDOCK: A protein-protein docking approach based on biochemical or biophysical information. J. Am. Chem. Soc. *125*, 1731–1737.

Fak, J.J., Itkin, A., Ciobanu, D.D., Lin, E.C., Song, X.J., Chou, Y.T., Gierasch, L.M., and Hunt, J.F. (2004). Nucleotide exchange from the high-affinity ATP-binding site in SecA is the rate-limiting step in the ATPase cycle of the soluble enzyme and occurs through a specialized conformational state. Biochemistry *43*, 7307–7327.

Fekkes, P., van der Does, C., and Driessen, A.J. (1997). The molecular chaperone SecB is released from the carboxy-terminus of SecA during initiation of precursor protein translocation. EMBO J. *16*, 6105–6113.

Gierasch, L.M. (1989). Signal sequences. Biochemistry *28*, 923–930.

Gross, J.D., Moerke, N.J., von der Haar, T., Lugovskoy, A.A., Sachs, A.B., McCarthy, J.E., and Wagner, G. (2003). Ribosome loading onto the mRNA cap is driven by conformational coupling between eIF4G and eIF4E. Cell *115*, 739–750.

Hegde, R.S., and Bernstein, H.D. (2006). The surprising complexity of signal sequences. Trends Biochem. Sci. *31*, 563–571.

Hunt, J.F., Weinkauf, S., Henry, L., Fak, J.J., McNicholas, P., Oliver, D.B., and Deisenhofer, J. (2002). Nucleotide control of interdomain interactions in the conformational reaction cycle of SecA. Science *297*, 2018–2026.

Iwahara, J., and Clore, G.M. (2006). Detecting transient intermediates in macromolecular binding by paramagnetic NMR. Nature *440*, 1227–1230.

Karamanou, S., Gouridis, G., Papanikou, E., Sianidis, G., Gelis, I., Keramisanou, D., Vrontou, E., Kalodimos, C.G., and Economou, A. (2007). Preprotein-controlled catalysis in the helicase motor of SecA. EMBO J. *26*, 2904–2914.

Karamyshev, A.L., and Johnson, A.E. (2005). Selective SecA association with signal sequences in ribosome-bound nascent chains - A potential role for SecA in ribosome targeting to the bacterial membrane. J. Biol. Chem. *280*, 37930–37940.

Keramisanou, D., Biris, N., Gelis, I., Sianidis, G., Karamanou, S., Economou, A., and Kalodimos, C.G. (2006). Disorder-order folding transitions underlie catalysis in the helicase motor of SecA. Nat. Struct. Mol. Biol. *13*, 594–602.

Kimura, E., Akita, M., Matsuyama, S., and Mizushima, S. (1991). Determination of a region in SecA that interacts with presecretory proteins in Escherichia coli. J. Biol. Chem. *266*, 6600–6606.

Kourtz, L., and Oliver, D. (2000). Tyr-326 plays a critical role in controlling SecA-preprotein interaction. Mol. Microbiol. *37*, 1342–1356.

Lill, R., Dowhan, W., and Wickner, W. (1990). The ATPase activity of SecA is regulated by acidic phospholipids, SecY, and the leader and mature domains of precursor proteins. Cell *60*, 271–280.

Matsuo, H., Walters, K.J., Teruya, K., Tanaka, T., Gassner, G.T., Lippard, S.J., Kyogoku, Y., and Wagner, G. (1999). Identification by NMR spectroscopy of residues at contact surfaces in large, slowly exchanging macromolecular complexes. J. Am. Chem. Soc. *121*, 9903–9904.

Mitra, K., Frank, J., and Driessen, A. (2006). Co- and post-translational translocation through the protein-conducting channel: Analogous mechanisms at work? Nat. Struct. Mol. Biol. *13*, 957–964.

Mori, H., Araki, M., Hikita, C., Tagaya, M., and Mizushima, S. (1997). The hydrophobic region of signal peptides is involved in the interaction with membrane-bound SecA. Biochim. Biophys. Acta *1326*, 23–36.

Mori, H., and Ito, K. (2006). Different modes of SecY-SecA interactions revealed by site-directed in vivo photo-cross-linking. Proc. Natl. Acad. Sci. USA *103*, 16159–16164.

Musial-Siwek, M., Rusch, S.L., and Kendall, D.A. (2007). Selective photoaffinity labeling identifies the signal peptide binding domain on SecA. J. Mol. Biol. *365*, 637–648.

Osborne, A.R., Clemons, W.M., Jr., and Rapoport, T.A. (2004). A large conformational change of the translocation ATPase SecA. Proc. Natl. Acad. Sci. USA *101*, 10937–10942.

Osborne, A.R., Rapoport, T.A., and van den Berg, B. (2005). Protein translocation by the Sec61/Secy channel. Annu. Rev. Cell Dev. Biol. *21*, 529–550.

Osborne, A.R., and Rapoport, T.A. (2007). Protein translocation is mediated by oligomers of the SecY complex with one SecY copy forming the channel. Cell *129*, 97–110.

Papanikolau, Y., Papadovasilaki, M., Ravelli, R.B., McCarthy, A.A., Cusack, S., Economou, A., and Petratos, K. (2007). Structure of dimeric SecA, the Escherichia coli preprotein translocase motor. J. Mol. Biol. *366*, 1545–1557.

Papanikou, E., Karamanou, S., Baud, C., Frank, M., Sianidis, G., Keramisanou, D., Kalodimos, C.G., Kuhn, A., and Economou, A. (2005). Identification of the preprotein binding domain of SecA. J. Biol. Chem. *280*, 43209–43217.

Randall, L.L., and Hardy, S.J. (2002). SecB, one small chaperone in the complex milieu of the cell. Cell. Mol. Life Sci. *59*, 1617–1623.

Randall, L.L., Topping, T.B., Hardy, S.J., Pavlov, M.Y., Freistroffer, D.V., and Ehrenberg, M. (1997). Binding of SecB to ribosome-bound polypeptides has the same characteristics as binding to full-length, denatured proteins. Proc. Natl. Acad. Sci. USA *94*, 802–807.

Roosild, T.P., Greenwald, J., Vega, M., Castronovo, S., Riek, R., and Choe, S. (2005). NMR structure of Mistic, a membrane-integrating protein for membrane protein expression. Science *307*, 1317–1321.

Schiebel, E., Driessen, A.J., Hartl, F.U., and Wickner, W. (1991). Delta mu H+ and ATP function at different steps of the catalytic cycle of preprotein translocase. Cell *64*, 927–939.

Sengoku, T., Nureki, O., Nakamura, A., Kobayashi, S., and Yokoyama, S. (2006). Structural basis for RNA unwinding by the DEAD-box protein Drosophila Vasa. Cell *125*, 287–300.

Sharma, V., Arockiasamy, A., Ronning, D.R., Savva, C.G., Holzenburg, A., Braunstein, M., Jacobs, W.R., Jr., and Sacchettini, J.C. (2003). Crystal structure of Mycobacterium tuberculosis SecA, a preprotein translocating ATPase. Proc. Natl. Acad. Sci. USA *100*, 2243–2248.

Sianidis, G., Karamanou, S., Vrontou, E., Boulias, K., Repanas, K., Kyrpides, N., Politou, A.S., and Economou, A. (2001). Cross-talk between catalytic and regulatory elements in a DEAD motor domain is essential for SecA function. EMBO J. *20*, 961–970.

Sprangers, R., and Kay, L.E. (2007). Quantitative dynamics and binding studies of the 20S proteasome by NMR. Nature *445*, 618–622.

Sprangers, R., Velyvis, A., and Kay, L.E. (2007). Solution NMR of supramolecular complexes: Providing new insights into function. Nat. Methods *4*, 697–703.

Tang, C., Iwahara, J., and Clore, G.M. (2006). Visualization of transient encounter complexes in protein-protein association. Nature *444*, 383–386.

Triplett, T.L., Sgrignoli, A.R., Gao, F.B., Yang, Y.B., Tai, P.C., and Gierasch, L.M. (2001). Functional signal peptides bind a soluble N-terminal fragment of SecA and inhibit its ATPase activity. J. Biol. Chem. *276*, 19648–19655.

Ureta, A.R., Endres, R.G., Wingreen, N.S., and Silhavy, T.J. (2007). Kinetic analysis of the assembly of the outer membrane protein LamB in Escherichia coli mutants each lacking a secretion or targeting factor in a different cellular compartment. J. Bacteriol. *189*, 446–454.

Van den Berg, B., Clemons, W.M., Jr., Collinson, I., Modis, Y., Hartmann, E., Harrison, S.C., and Rapoport, T.A. (2004). X-ray structure of a protein-conducting channel. Nature *427*, 36–44.

Vassylyev, D.G., Mori, H., Vassylyeva, M.N., Tsukazaki, T., Kimura, Y., Tahirov, T.H., and Ito, K. (2006). Crystal structure of the translocation ATPase SecA from thermus thermophilus reveals a parallel, head-to-head dimer. J. Mol. Biol. *364*, 248–258.

Volkov, A.N., Worrall, J.A., Holtzmann, E., and Ubbink, M. (2006). Solution structure and dynamics of the complex between cytochrome c and cytochrome c peroxidase determined by paramagnetic NMR. Proc. Natl. Acad. Sci. USA *103*, 18945–18950.

von Heijne, G. (1985). Signal sequences. The limits of variation. J. Mol. Biol. *184*, 99–105.

Zhou, J., and Xu, Z. (2003). Structural determinants of SecB recognition by SecA in bacterial protein translocation. Nat. Struct. Biol. *10*, 942–947.

Wang, Z., Jones, J.D., Rizo, J., and Gierasch, L.M. (1993). Membrane-bound conformation of a signal peptide: a transferred nuclear Overhauser effect analysis. Biochemistry *32*, 13991–13999.

Wang, L., Miller, A., Rusch, S.L., and Kendall, D.A. (2004). Demonstration of a specific Escherichia coli SecY-signal peptide interaction. Biochemistry *43*, 13185–13192.

Wang, L., Miller, A., and Kendall, D.A. (2000). Signal peptide determinants of SecA binding and stimulation of ATPase activity. J. Biol. Chem. *275*, 10154–10159.

Wickner, W., and Schekman, R. (2005). Protein translocation across biological membranes. Science *310*, 1452–1456.

Accession Numbers

Structural coordinates are deposited in the Protein Data Bank (ID 2VDA).